

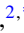



Flying-qubit control via a three-level atom with tunable waveguide couplings

Wenlong Li ¹, Xue Dong ¹, Guofeng Zhang ^{2,*} and Re-Bing Wu ^{1,†}

¹*Center for Intelligent and Networked Systems, Department of Automation, Tsinghua University, Beijing 100084, China*

²*Department of Applied Mathematics, The Hong Kong Polytechnic University, Kowloon 999077, Hong Kong, China and The Hong Kong Polytechnic University Shenzhen Research Institute, Shenzhen, Guang Dong 518057, China*



(Received 28 May 2022; revised 19 September 2022; accepted 20 September 2022; published 18 October 2022)

The control of flying qubits is at the core of quantum networks. When the flying qubits are carried by single-photon fields, the control involves not only their logical states but also their shapes. In this paper we explore a variety of flying-qubit control problems using a three-level atom with time-varying tunable couplings to two input-output channels. It is shown that one can tune the couplings of a Λ -type atom to distribute a single photon into the two channels with arbitrary shapes, or use a Λ -type atom or a V -type atom to catch an arbitrary-shape distributed single photon. The Λ -type atom can also be designed to transfer a flying qubit from one channel to the other, with both the central frequency and the photon shape being converted. With a Ξ -type atom, one can shape a pair of correlated photons via cascaded emission. In all cases, analytical formulas are derived for the coupling functions to fulfill these control tasks. Their correlation properties and physical limitations are discussed as well. These results provide useful control protocols for high-fidelity quantum information transmission over complex quantum networks.

DOI: [10.1103/PhysRevB.106.134305](https://doi.org/10.1103/PhysRevB.106.134305)

I. INTRODUCTION

The engineering of flying qubits is fundamentally important in coherent information transmission over quantum networks [1–6]. Usually, the logical states of flying qubits are encoded by the number or polarization of photons contained in a pulsed electromagnetic field. Moreover, since the photon field often involves a continuous band of modes, its spectrum (or equivalently its temporal shape) is also to be well shaped so as to physically match the receiver quantum nodes [7–9].

The control of flying qubits must be actuated by some manipulatable standing quantum system (i.e., an atom). In the view of quantum input-output theory [10–12], the incoming and outgoing flying qubits form the quantum input and output of the standing quantum system. Roughly speaking, we may encounter the following three classes of control tasks: (1) the generation of flying qubits with vacuum quantum inputs [13–19], (2) the catching of flying qubits that yields vacuum quantum outputs [7–9, 15, 20–22], and (3) the transformation of flying qubits with both nonvacuum quantum inputs and outputs [18, 23–27].

To fulfill the above control tasks, the actuating standing quantum systems should be properly structured. For the generation or catching of arbitrary-shape single flying qubits, it is sufficient to apply a simple two-level atom [9, 28, 29]. However, when processing multiple flying qubits or routing flying qubits between different channels [30–32], multilevel atoms are required [33–36]. As the simplest extension, a three-level atom that is simultaneously coupled to two channels

may convert flying qubits from one channel to the other or distribute an entangled pair of flying qubits between the two channels.

In this paper we are mainly concerned with microwave flying-qubit controls with an artificial three-level atom in superconducting quantum circuits, because their couplings to cavities or waveguides can be flexibly tuned in real time [37–39]. All kinds of three-level artificial atoms can be realized, including the Λ type [40], the Ξ type [41], the V type [42], and the cyclic Δ type [37] that does not exist in natural atoms. The Λ -type atoms were proposed for the generation of persistent single photons [43, 44], the nonreciprocal routing of single photons among two coupled chiral waveguides [45], and the few-photon scattering processes [26], while Ξ -type atoms can be taken as transistors for switching single photons scattered by the atom [46]. One can also apply the Δ -type atom to the generation of microwave photon pairs [47, 48] and the routing of single photons [49].

To our knowledge, little attention has been paid to the control of flying-qubit shape with three-level atoms using tunable couplings. In the literature, various approaches have been proposed to model such dynamical processes in the frequency domain, including the master equations [50], quantum Langevin equations [10], and quantum trajectories [51, 52]. However, these approaches cannot be directly applied when the underlying control processes involve time-varying parameters (e.g., tunable coupling strength). Such systems have to be modeled in the time domain using approaches using quantum scattering analysis [18, 19, 23, 24, 53, 54] or quantum stochastic differential equations (QSDEs) [28, 55]. Both approaches lead to a nonunitary Schrödinger equation of the standing quantum system that characterizes the quantum trajectories along which single photons are randomly emitted.

*guofeng.zhang@polyu.edu.hk

†rbwu@tsinghua.edu.cn

Here we will explore a variety of flying-qubit control problems using a three-level atom [56] with tunable couplings to two quantum input-output channels. Based on the QSDE-based approach, we will derive analytic conditions for the time-varying coupling strengths and detuning frequencies to generate, catch, or convert flying qubits with different types of three-level atoms. Their scattering properties, physical limitations, and the second-order correlation [57] will be discussed as well.

The remainder of this paper is organized as follows. Section II describes the flying-qubit control model based on our previous work [28,29]. In Sec. III we design control protocols for the generation of entangled flying qubits and cascaded generation of flying-qubit pairs, following which the catching and conversion of flying qubits are discussed in Secs. IV and V, respectively. In Sec. VI the second-order correlation of the output fields will be analyzed. Finally, the conclusion is drawn in Sec. VII.

II. THE MODEL OF FLYING-QUBIT CONTROL SYSTEMS

In this section we will introduce the dynamical model for analyzing the controlled flying-qubit input-output processes with a three-level atom.

A. The representation of flying-qubit states

Consider flying qubits carried by quantized fields traveling in a one-dimensional nondispersive waveguide, and it is assumed that the fields have fixed polarization direction. The logical states of the flying qubits are encoded by the number of photons contained in the field, e.g., $|0\rangle$ and $|1\rangle$ are represented by the field's vacuum state and single-photon state, respectively. In addition to the logical state, the shape of the field, or equivalently the distribution of the photon field over different modes, is also important for efficient transmission of flying qubits.

To define the state of such quantized traveling fields, we first introduce the dimensionless field operator

$$b(x, t) = \frac{1}{\sqrt{2\pi}} \int_{-\infty}^{+\infty} d\omega e^{-i\omega(t-x/c)} b_0(\omega), \quad (1)$$

where t and x are the time and position of observation in the waveguide; and $b_0(\omega)$ is the annihilation operator of the optical mode with frequency ω at the reference point ($x = 0, t = 0$). The propagation speed c is constant in the nondispersive waveguide, and hence the field is invariant under the translation transformation $(t, x) \rightarrow (t + t', x + ct')$. Regarding this, it is equivalent to represent the field either in temporal form (i.e., observing the field at a fixed position) or spatial form (i.e., observing the field at a fixed time instant). Since the analysis of flying qubits in this paper is dependent on the dynamics of the standing three-level atom that is coupled to the waveguide at $x = 0$, we will adopt the temporal form $b(t) \triangleq b(x = 0, t)$ in the following discussions.

Using the field operator, we can describe a pulsed single-photon state as follows [12,24]:

$$|1_\xi\rangle = \int_{-\infty}^{+\infty} \xi(\tau) b^\dagger(\tau) |\text{vac}\rangle d\tau, \quad (2)$$

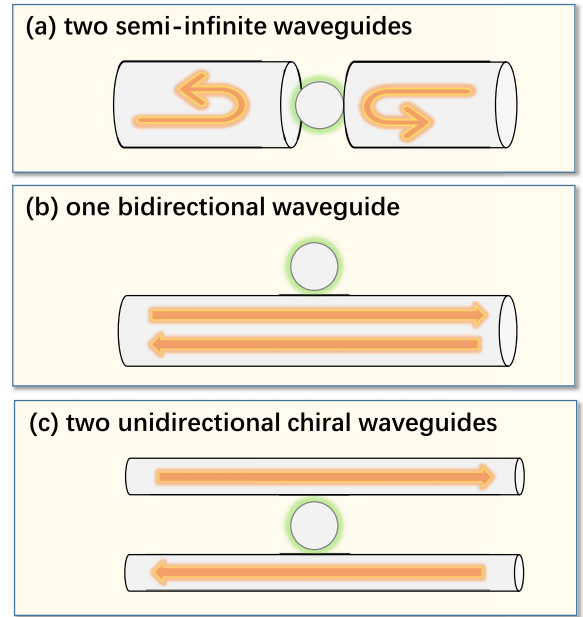


FIG. 1. Schematics of a standing quantum system with two coupled quantum input-output channels that may physically correspond to (a) two semi-infinite waveguides, (b) one bidirectional waveguide, or (c) two unidirectional chiral waveguides.

where the shape function $\xi(t)$ represents the probability amplitude of finding a photon at moment t , and the preservation of the overall probability requires that $\xi(t)$ be normalized, i.e., $\int_{-\infty}^{+\infty} |\xi(\tau)|^2 d\tau = 1$.

The single-photon field can also be distributed in multiple channels, which can be represented by the following superposition of m single-photon components:

$$|1_\xi\rangle = \sum_{j=1}^m \int_{-\infty}^{+\infty} \xi_j(\tau) b_j^\dagger(\tau) |\text{vac}\rangle d\tau, \quad (3)$$

where $b_j^\dagger(\tau)$ and $\xi_j(\tau)$ are the field operator and photon shape function in the j th channel, respectively.

More generally, we can define n -photon states in m channels as follows:

$$|n_\xi\rangle = \sum_{j_1, \dots, j_n=1}^m \int_{-\infty}^{+\infty} d\tau_n \int_{-\infty}^{\tau_n} d\tau_{n-1} \cdots \int_{-\infty}^{\tau_2} d\tau_1 \times \xi_{j_1, \dots, j_n}(\tau_1, \dots, \tau_n) b_{j_n}^\dagger(\tau_n) \cdots b_{j_1}^\dagger(\tau_1) |\text{vac}\rangle, \quad (4)$$

where the shape function $\xi_{j_1, \dots, j_n}(\tau_1, \dots, \tau_n)$ indicates the probability density amplitude of generating the k th photon in the j_k th channel at time τ_k . For notational consistency, we denote the shape function with zero photon as ξ that does not have any superscripts or subscripts.

B. The computation of outgoing flying-qubit states

Consider a three-level atom that is coupled to two quantum input-output channels. Let $|g\rangle$, $|e\rangle$, and $|f\rangle$ be the atom's eigenstates, where $|f\rangle$ is the highest excited state, and \mathcal{H} is the Hilbert space they span. As is shown in Fig. 1, the two channels can be physically realized by two

semi-infinite waveguides, a bidirectional waveguide, or two unidirectional waveguides. Throughout this paper we take the third scenario for the description of a problem setup, but the obtained results can be directly extended to the other two scenarios.

To analyze the underlying quantum input-output processes, we generalize the above flying-qubit state representation to the joint state of the interacting atom-waveguide system, as follows:

$$|\Psi(t)\rangle = \sum_{n=0}^{\infty} \sum_{j_1, \dots, j_n=1}^2 \int_{-\infty}^t d\tau_n \int_{-\infty}^{\tau_n} d\tau_{n-1} \cdots \int_{-\infty}^{\tau_2} d\tau_1 \times |\psi_{j_1, \dots, j_n}(\tau_1, \dots, \tau_n|t)\rangle \otimes b_{j_n}^\dagger(\tau_n) \cdots b_{j_1}^\dagger(\tau_1) |\text{vac}\rangle, \quad (5)$$

where $|\psi_{j_1, \dots, j_n}(\tau_1, \dots, \tau_n|t)\rangle \in \mathcal{H}$ is the atom's associated state at time t when n photons are observed at moments $\tau_1 \leq \dots \leq \tau_n$ in the j_1 th, \dots , j_n th channels, respectively. Note that each $|\psi_{j_1, \dots, j_n}(\tau_1, \dots, \tau_n|t)\rangle$ is generally unnormalized, but the total state $|\Psi(t)\rangle$ is always normalized.

Assume that the quantum input field (i.e., incoming flying qubits) is in the vacuum state $|\text{vac}\rangle$, and the atom is initially prepared at state $|\psi(-\infty)\rangle = |\psi_0\rangle$. In our previous studies [28,29] it is shown that the unitary time evolution of the joint state $|\Psi(t)\rangle$ can be decomposed into a series of differential equations for the associated states $|\psi_{j_1, \dots, j_n}(\tau_1, \dots, \tau_n|t)\rangle$, which all obey the following nonunitary evolution equation of

$V(t)$ on \mathcal{H} [58]:

$$\dot{V}(t) = \left[-iH(t) - \frac{1}{2} \sum_{j=1}^2 L_j^\dagger(t) L_j(t) \right] V(t), \quad (6)$$

where $V(-\infty) = \mathbb{I}$, $H(t)$ is the atom's Hamiltonian including its internal and interaction parts, and $L_i(t)$ ($i = 1, 2$) is its coupling operator to the j th channel. The evolution equation is nonunitary because the atom experiences Markovian open dynamics with the coupled photon fields being its reservoirs.

Using the evolution operator $V(t)$, each $|\psi_{j_1, \dots, j_n}(\tau_1, \dots, \tau_n|t)\rangle$ can be calculated as follows:

$$|\psi_{j_1, \dots, j_n}(\tau_1, \dots, \tau_n|t)\rangle = V(t) \tilde{L}_{j_n}(\tau_n) \cdots \tilde{L}_{j_1}(\tau_1) |\psi_0\rangle, \quad (7)$$

where $\tilde{L}_{j_i}(\tau_i) = V^{-1}(\tau_i) L_{j_i}(\tau_i) V(\tau_i)$.

The outgoing flying-qubit state can be extracted from the asymptotic limit of $|\Psi(t)\rangle$ when $t \rightarrow \infty$. Owing to the decaying nature of $V(t)$, each component $|\psi_{j_1, \dots, j_n}(\tau_1, \dots, \tau_n|t)\rangle$ must decay to either $|g\rangle$ or $|e\rangle$, and can thus be decomposed as

$$|\psi_{j_1, \dots, j_n}(\tau_1, \dots, \tau_n|\infty)\rangle = \xi_{j_1, \dots, j_n}^g(\tau_1, \dots, \tau_n) |g\rangle + \xi_{j_1, \dots, j_n}^e(\tau_1, \dots, \tau_n) |e\rangle. \quad (8)$$

Thus, under the asymptotic limit, we can reexpress the joint state as

$$|\Psi(\infty)\rangle = |g\rangle \otimes \left[\sum_{n=0}^{\infty} \sum_{j_1, \dots, j_n=1}^2 \int_{-\infty}^{\infty} d\tau_n \cdots \int_{-\infty}^{\tau_2} d\tau_1 \xi_{j_1, \dots, j_n}^g(\tau_1, \dots, \tau_n) b_{j_n}^\dagger(\tau_n) \cdots b_{j_1}^\dagger(\tau_1) |\text{vac}\rangle \right] + |e\rangle \otimes \left[\sum_{n=0}^{\infty} \sum_{j_1, \dots, j_n=1}^2 \int_{-\infty}^{\infty} d\tau_n \cdots \int_{-\infty}^{\tau_2} d\tau_1 \xi_{j_1, \dots, j_n}^e(\tau_1, \dots, \tau_n) b_{j_n}^\dagger(\tau_n) \cdots b_{j_1}^\dagger(\tau_1) |\text{vac}\rangle \right], \quad (9)$$

in which the summations in the brackets represent the state of the emitted photon field when the atom decays to $|g\rangle$ or $|e\rangle$. In particular, when the number of excitation numbers is preserved, the summations usually contain a finite number of terms and hence can be explicitly calculated to analyze the control processes.

When the quantum input of some channel is in a nonvacuum state, we can generalize the above procedure by cascading an ancillary system that generates the quantum input (see Fig. 2). The resulting composite system thus receives vacuum quantum inputs and the above procedure can be directly applied. Concidentally, suppose that the nonvacuum quantum input is fed into the first channel. Let $H_A(t)$ and $L_A(t)$ be the Hamiltonian and the coupling operator of the ancillary system A, which can be artificially chosen according to the desired input state $|1_\xi\rangle$.

For example, we can use a two-level system with tunable coupling to generate arbitrary-shape single photons. According to the (S, L, H) formula [59], the equivalent Hamiltonian of the joint system is

$$\tilde{H}(t) = H_A(t) \otimes \mathbb{I} + \mathbb{I}_A \otimes H(t) + \frac{1}{2i} [L_1^\dagger(t) L_A(t) - L_A^\dagger(t) L_1(t)], \quad (10)$$

and the equivalent coupling operators are

$$\tilde{L}_1(t) = \mathbb{I}_A \otimes L_1(t) + L_A(t) \otimes \mathbb{I}, \quad (11a)$$

$$\tilde{L}_2(t) = \mathbb{I}_A \otimes L_2(t). \quad (11b)$$

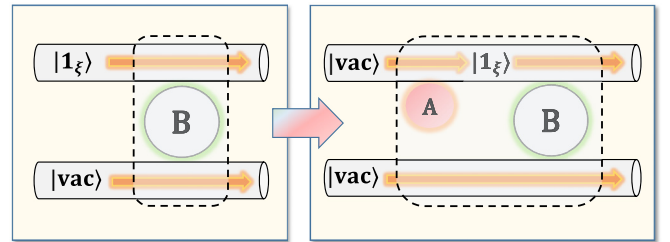


FIG. 2. Schematics for transforming a nonvacuum input system (the box on the left) to an equivalent system with vacuum input (the box on the right). The single-photon input state $|1_\xi\rangle$ is generated by a properly designed ancillary system A.

The equivalent $\bar{H}(t)$ and $\bar{L}_j(t)$ can then be applied to construct the nonunitary evolution equation (6) for the calculation of output fields. The same procedure can be done when the second channel or both channels have nonvacuum inputs.

C. Existing results on flying-qubit control with two-level atoms

Before studying flying-qubit control actuated by a three-level atom, we briefly review the known results with a two-level atom.

Suppose that the internal Hamiltonian of the two-level system is $H(t) = \epsilon(t)\sigma_z$, where $\epsilon(t)$ is the detuning angular frequency between the atomic transition frequency and the central frequency of the field in the channel. The coupling operator is $L(t) = \sqrt{\gamma(t)}\sigma_-$, where σ_- is the standard Pauli lowering operator. In previous works [9,28,29], it is derived that, to generate a single-photon pulse $\xi(t) = |\xi(t)|e^{-i\phi(t)}$ from an excited two-level atom, the coupling function should be set to

$$\bar{\gamma}(t) = \frac{|\xi(t)|^2}{\int_t^\infty |\xi(s)|^2 ds}, \quad (12)$$

and the detuning frequency needs to match the phase matching condition $\epsilon(t) = \dot{\phi}(t)$, where $\phi(t)$ must start from $\phi(-\infty) = 0$. Hereafter, the double bars over $\gamma(t)$ are used to denote coupling functions associated with two-level atoms.

One can also derive that, to catch a single photon $|1_\xi\rangle$ with $\xi(t) = |\xi(t)|e^{-i\phi(t)}$, the coupling function $\gamma(t)$ should be set to [9]

$$\bar{\gamma}(t) = \frac{|\xi(t)|^2}{\int_{-\infty}^t |\xi(s)|^2 ds}, \quad (13)$$

while the same phase matching condition needs to be satisfied.

The above conditions for controlling flying qubits exhibit an elegant symmetry in that the integral in the denominator is performed over the entire future (i.e., $[t, \infty)$) when generating a single photon. Correspondingly, the integral is done over the entire past (i.e., $(-\infty, t]$) when catching a single photon.

III. THE GENERATION OF FLYING QUBITS WITH A THREE-LEVEL ATOM

In this section we will use the above flying-qubit control model to design control functions for generating flying qubits with a Λ -type or a Ξ -type atom.

A. Entangled flying qubits generated by a Λ -type atom

Consider a Λ -type atom that is coupled to two quantum channels (see Fig. 3). Being initially excited to the state $|f\rangle$, the atom will emit a single photon distributed into the two channels, forming a pair of flying qubits that are entangled with the atom after they leave. Their joint state can be written as

$$|\Psi(\infty)\rangle = \alpha_1|g\rangle \otimes |1_{\xi_1}\rangle|\text{vac}\rangle + \alpha_2|e\rangle \otimes |\text{vac}\rangle|1_{\xi_2}\rangle, \quad (14)$$

where the coefficients α_1 and α_2 are complex numbers and the shape functions $\xi_1(t)$ and $\xi_2(t)$ are normalized.

The coupling operators are in the following form:

$$L_1(t) = \sqrt{\gamma_1(t)}|g\rangle\langle f|, \quad L_2(t) = \sqrt{\gamma_2(t)}|e\rangle\langle f|, \quad (15)$$

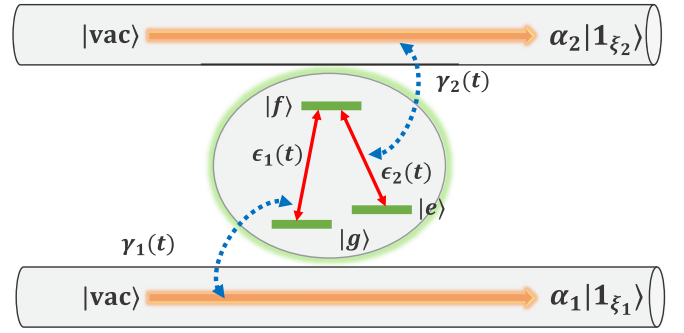


FIG. 3. Schematics for the generation of a distributed single photon with a Λ -type three-level atom, which forms a pair of flying qubits that is entangled with the atom at state $\alpha_1|g\rangle|1_{\xi_1}\rangle|\text{vac}\rangle + \alpha_2|e\rangle|\text{vac}\rangle|1_{\xi_2}\rangle$. Here $\epsilon_1(t)$ and $\epsilon_2(t)$ are the detunings between the central frequency of the incident field and the corresponding atomic transition frequencies, respectively, and $\gamma_1(t)$ and $\gamma_2(t)$ are the coupling functions.

where the tunable coupling functions $\gamma_1(t)$ and $\gamma_2(t)$ alter the instantaneous rate of field emission into the corresponding channels. In the rotating-wave frame, the system's Hamiltonian reads

$$H(t) = [\epsilon_1(t) + \epsilon_2(t)]|f\rangle\langle f|, \quad (16)$$

where $\epsilon_1(t)$ and $\epsilon_2(t)$ are the detuning angular frequencies between the transition frequencies and central frequencies of the channels. According to Eqs. (7)–(9), we can derive that (see Appendix A 1 for details), for arbitrary given coefficients α_1 and α_2 and shape functions $\xi_1(t)$ and $\xi_2(t)$, one can generate the entangled state (14) using the following coupling functions:

$$\gamma_1(t) = \frac{|\alpha_1\xi_1(t)|^2}{\int_t^\infty |\alpha_1\xi_1(s)|^2 ds + \int_t^\infty |\alpha_2\xi_2(s)|^2 ds}, \quad (17a)$$

$$\gamma_2(t) = \frac{|\alpha_2\xi_2(t)|^2}{\int_t^\infty |\alpha_1\xi_1(s)|^2 ds + \int_t^\infty |\alpha_2\xi_2(s)|^2 ds}, \quad (17b)$$

which have a common denominator because the coupling operators of the two channels share the excited state $|f\rangle$.

Let $\xi_j(t) = |\xi_j(t)|e^{-i\phi_j(t)}$ ($j = 1, 2$) with $\phi_j(t)$ being the phase of the shape function. To match the phases, the detuning frequencies should satisfy

$$\epsilon_1(t) + \epsilon_2(t) = \dot{\phi}_1(t) = \dot{\phi}_2(t), \quad (18)$$

where $\phi_1(-\infty) = \phi_2(-\infty) = 0$. This actually requires that $\xi_1(t)$ and $\xi_2(t)$ must have identical phase functions $\phi_1(t) = \phi_2(t)$.

The obtained solution (17) is closely related to the single-photon generation condition (12) with a two-level atom. They are similar in that both denominators represent the total number of photons to be released in the future. Because the number of excitation numbers (or energy) is preserved, the denominators are also equal to the remaining population of the initially excited state ($|e\rangle$ for the two-level atom and $|f\rangle$ for the three-level atom) at present time t .

For illustration, we simulate two typical classes of single-photon shape functions. In the first case we assume that both $\xi_1(t)$ and $\xi_2(t)$ are in the following exponentially

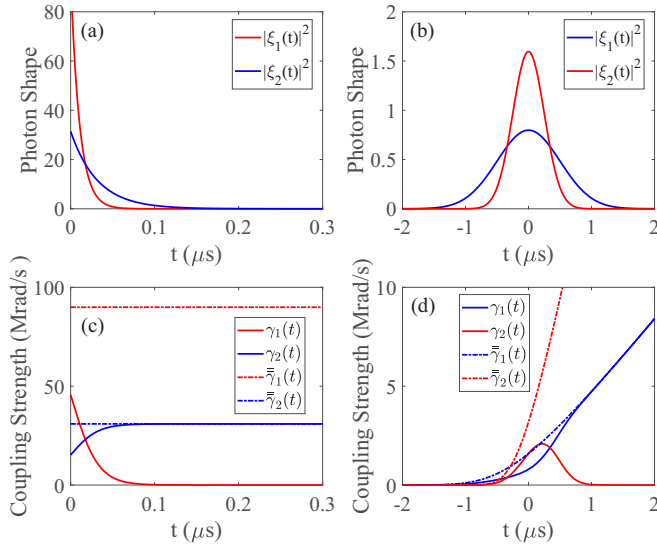


FIG. 4. The generation of a pair of flying qubits at the joint state as $\frac{1}{\sqrt{2}}(|g\rangle|1_{\xi_1}\rangle|\text{vac}\rangle + |e\rangle|\text{vac}\rangle|1_{\xi_2}\rangle)$ using a Λ -type atom. The output single photons have (a) exponentially decaying shapes or (b) Gaussian shapes, whose corresponding coupling strengths are shown in (c) and (d), respectively.

decaying form:

$$\xi_k(t) = \sqrt{\gamma_{ck}} e^{-\gamma_{ck}t/2}, \quad k = 1, 2, \quad (19)$$

where $\gamma_{c1}/2\pi = 15$ MHz and $\gamma_{c2}/2\pi = 5$ MHz. According to Eq. (17), it is easy to calculate that, to generate a pair of arbitrary-shape flying qubits with the above waveforms at the joint state as $\frac{1}{\sqrt{2}}(|g\rangle|1_{\xi_1}\rangle|\text{vac}\rangle + |e\rangle|\text{vac}\rangle|1_{\xi_2}\rangle)$, the coupling functions need to be

$$\gamma_1(t) = \frac{\gamma_{c1}}{1 + e^{(\gamma_{c1} - \gamma_{c2})t}}, \quad (20a)$$

$$\gamma_2(t) = \frac{\gamma_{c2}}{1 + e^{(\gamma_{c2} - \gamma_{c1})t}}. \quad (20b)$$

Recall that, according to Eq. (12), the coupling function for generating the two exponentially decaying waveforms with two-level atoms are $\bar{\gamma}_1(t) \equiv \gamma_{c1}$ and $\bar{\gamma}_2(t) \equiv \gamma_{c2}$, respectively. There is a competition between the photon emission in the two channels in that $\gamma_2(t)$ asymptotically approaches $\bar{\gamma}_2(t)$ but the more rapidly decaying $\gamma_1(t)$ gradually vanishes.

This competition also exists when the two single-photon shapes are both Gaussian functions:

$$\xi_k(t) = \left(\frac{\Omega_k^2}{2\pi}\right)^{1/4} e^{-\frac{\Omega_k t^2}{2}}, \quad k = 1, 2, \quad (21)$$

where Ω_k is the bandwidth of the frequency domain waveform corresponding to the single photon $\xi_k(t)$, $\Omega_1 = 2$ MHz and $\Omega_2 = 4$ MHz. We can see in Fig. 4(d) that, as predicted, the required coupling function $\gamma_1(t)$ approaches $\bar{\gamma}_1(t)$ because $\xi_1(t)$ decays more slowly, and $\gamma_2(t)$ gradually vanishes.

B. Cascaded generation of correlated flying qubits by a Ξ -type atom

Consider a Ξ -type atom shown in Fig. 5. When the atom is initially prepared at the excited state $|f\rangle$, a pair of single

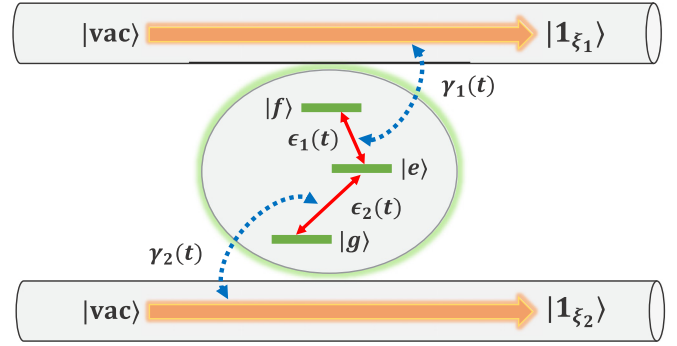


FIG. 5. Schematics for the generation of a pair of correlated single photons by a Ξ -type atom, including $|1_{\xi_1}\rangle$ in the first channel and $|1_{\xi_2}\rangle$ in the second channel. Here $\epsilon_1(t)$ and $\epsilon_2(t)$ are the detuning frequencies between the incident field and the $|f\rangle \leftrightarrow |e\rangle$ and $|e\rangle \leftrightarrow |g\rangle$ transition frequencies, respectively; $\gamma_1(t)$ and $\gamma_2(t)$ are the coupling coefficients between the Ξ -type atom and the channels.

photons will be sequentially emitted into the first and the second channels. We seek proper coupling functions $\gamma_1(t)$ and $\gamma_2(t)$ to shape $|\xi_1(t)|^2$ and $|\xi_2(t)|^2$ as demanded. The underlying internal Hamiltonian and coupling operators of the Ξ -type atom are as follows:

$$H(t) = \epsilon_1(t)|f\rangle\langle f| + \epsilon_2(t)|e\rangle\langle e|, \quad (22)$$

$$L_1(t) = \sqrt{\gamma_1(t)}|e\rangle\langle f|, \quad (23)$$

$$L_2(t) = \sqrt{\gamma_2(t)}|g\rangle\langle e|. \quad (24)$$

Because the three-level atom eventually decays the ground state $|g\rangle$, the yielded two-photon wave packet can be calculated as

$$\xi_{1,2}^g(\tau_1, \tau_2) = \sqrt{\gamma_1(\tau_1)\gamma_2(\tau_2)} e^{-\frac{1}{2} \int_{-\infty}^{\tau_1} \gamma_1(s) ds - \frac{1}{2} \int_{\tau_1}^{\tau_2} \gamma_2(s) ds} \times e^{-i \int_{-\infty}^{\tau_1} \epsilon_1(s) ds - i \int_{\tau_1}^{\tau_2} \epsilon_2(s) ds}, \quad (25)$$

which remains in Eq. (8). Generally, the correlated two-photon generally cannot be decomposed into the direct product $|1_{\xi_1}\rangle \otimes |1_{\xi_2}\rangle$ of two single-photon states. Thus, the actually observed single-photon wave packets in each channel are the corresponding marginal probability distribution functions:

$$|\xi_1(\tau_1)|^2 = \int_{\tau_1}^{\infty} |\xi_{1,2}^g(\tau_1, \tau_2)|^2 d\tau_2, \quad (26)$$

$$|\xi_2(\tau_2)|^2 = \int_{-\infty}^{\tau_2} |\xi_{1,2}^g(\tau_1, \tau_2)|^2 d\tau_1. \quad (27)$$

Consequently, $\xi_1(t)$ and $\xi_2(t)$ do not possess definite phases $\phi_1(t)$ and $\phi_2(t)$ as the two photons are not separable.

From the derivation in Appendix A 2 for details, we have

$$\gamma_1(t) = \frac{|\xi_1(t)|^2}{\int_t^{\infty} |\xi_1(s)|^2 ds}, \quad (28a)$$

$$\gamma_2(t) = \frac{|\xi_2(t)|^2}{\int_t^{\infty} |\xi_2(s)|^2 ds - \int_t^{\infty} |\xi_1(s)|^2 ds}. \quad (28b)$$

The solution (28) indicates that $\gamma_1(t)$ is only dependent on the shape function $|\xi_1(t)|^2$ and thus its design can be treated as

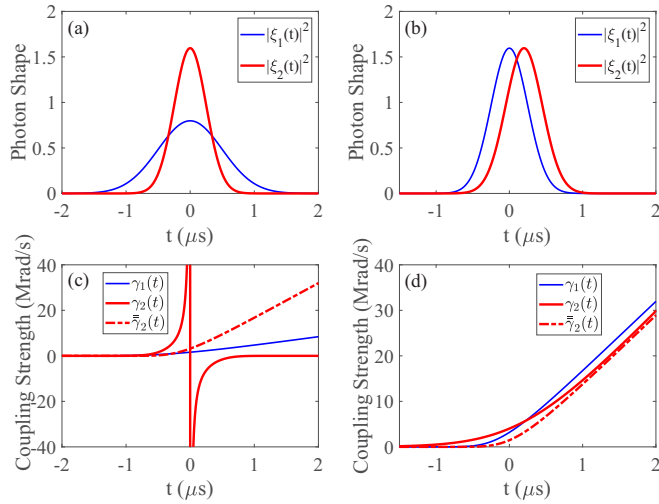


FIG. 6. The generation of a pair of correlated single photons using a Ξ -type atom. The photon shapes $\xi_1(t)$ and $\xi_2(t)$ are with (a) different Gaussian shapes both centered at $t = 0$ or (b) identical Gaussian shapes whose centers are separated by $\Delta = 0.2 \mu\text{s}$. The corresponding coupling strengths are shown in (c) and (d), respectively.

that with a two-level atom. However, the design of $\gamma_2(t)$ is not only dependent on the shape function $|\xi_2(t)|^2$ but also on $|\xi_1(t)|^2$ of the previously emitted photon.

The observed population rule in the above discussion can be verified here as the denominator of (Eq. (28a)) is equal to the current population of $|f\rangle$, whose decay leads to the emission of the first photon. Also, owing to the conservation of energy, the denominator of (Eq. (28b)) represents the accumulated population of the state $|e\rangle$ that is associated with the emission of the second photon, as it is equal to the difference between the energies dumped from the upper level $|f\rangle$ and to the lower level $|g\rangle$ indicated by the denominator.

Due to the passivity of the control system, the energy dumped to $|g\rangle$ can only come from the energy dumped from $|f\rangle$, and hence the following physical realizability condition must be held:

$$\int_t^\infty |\xi_2(s)|^2 ds > \int_t^\infty |\xi_1(s)|^2 ds, \quad \forall t > 0, \quad (29)$$

which is also demanded by positivity of $\gamma_2(t)$ according to (Eq. (28b)). This condition implies that the tail area of $|\xi_2(t)|^2$ must be always greater than that of $|\xi_1(t)|^2$, and hence $|\xi_1(t)|^2$ should decay more quickly.

We illustrate the above result with two representative examples of Gaussian photon pulses. In the first example, the two Gaussian pulses have different widths and identical peak times. As shown in Figs. 6(a) and 6(c), the tail areas of $|\xi_2(t)|^2$ are initially greater than that of $|\xi_1(t)|^2$, but becomes smaller later. This leads to the singularity of $\gamma_2(t)$ at the peak time and nonphysical negativity after that, which indicates that such photon shapes are not physically realizable by tunable couplings.

In the second example, the two photons have identical Gaussian shapes, but the second photon is behind the first with

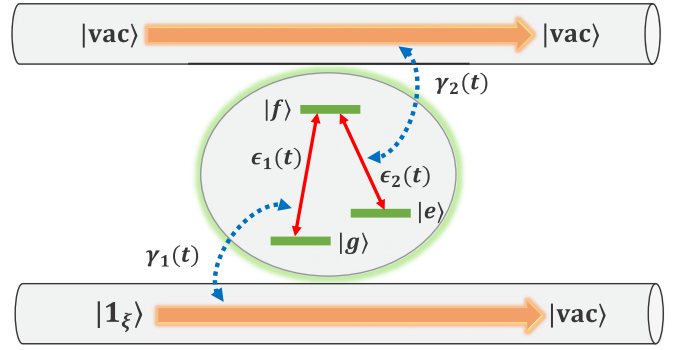


FIG. 7. Schematics for catching a flying qubit at state $|1_\xi\rangle|\text{vac}\rangle$ by a Λ -type atom at state $|g\rangle$. Here $\epsilon_1(t)$ and $\epsilon_2(t)$ are the detuning frequencies between the incident field and the $|f\rangle \leftrightarrow |g\rangle$ and $|f\rangle \leftrightarrow |e\rangle$ transition frequencies, respectively. $\gamma_1(t)$ and $\gamma_2(t)$ are the coupling coefficients between the Λ -type atom and the channels.

a time delay Δ , as follows:

$$\begin{aligned} |\xi_1(t)| &= \left(\frac{\Omega^2}{2\pi}\right)^{1/4} e^{-[\frac{\Omega t}{2}]^2}, \\ |\xi_2(t)| &= \left(\frac{\Omega^2}{2\pi}\right)^{1/4} e^{-[\frac{\Omega(t-\Delta)}{2}]^2}, \end{aligned} \quad (30)$$

in which $\Omega = 4 \text{ MHz}$ and $\Delta = 0.2 \mu\text{s}$. As are shown in Figs. 6(b) and 6(d), $\gamma_2(t)$ is physically realizable because the condition (29) holds. Because the tail area of $|\xi_1(t)|^2$ decays more quickly, $\gamma_2(t)$ asymptotically approaches $\bar{\gamma}_2(t)$ which is associated with a two-level atom.

IV. THE CATCHING OF FLYING QUBITS BY A THREE-LEVEL ATOM

Let us first consider the Λ -type atom shown in Fig. 7. When the atom is initially prepared at the state $|g\rangle$, we wish to catch a single photon $|1_\xi\rangle$ from the first channel, i.e., finding proper control functions such that the outputs of both channels are empty, and the atom's state transits from $|g\rangle$ to $|f\rangle$. Assuming that $\xi(t) = |\xi(t)|e^{-i\phi(t)}$, we can introduce an ancillary system A to generate $|1_\xi\rangle$, and apply Eqs. (7)–(9) to the joint standing system. It can be derived that the coupling function and detuning of the first channel must be

$$\gamma_1(t) = \frac{|\dot{\xi}(t)|^2}{\int_{-\infty}^t |\xi(s)|^2 ds}, \quad \epsilon_1(t) = \dot{\phi}(t). \quad (31)$$

Meanwhile, the coupling to the second channel must be turned off, i.e., $\gamma_2(t) \equiv 0$, so as to prevent the leakage of the photon into the second channel. (The details of its derivation can be found in Appendix A 3.) Thus, the design of such controls is exactly the same as that with a two-level atom.

We can also use a V -type atom to catch a distributed single photon. As is shown in Fig. 8, the photon fields coming from both channels, forming an entangled state $\alpha_1|1_\xi\rangle|\text{vac}\rangle + \alpha_2|\text{vac}\rangle|1_\xi\rangle$, where $\xi_k(t) = |\xi_k(t)|e^{-i\phi_k(t)}$ ($k = 1, 2$). When the atom is initially prepared at the ground state $|g\rangle$, we can prove that the coupling functions and detuning frequencies for

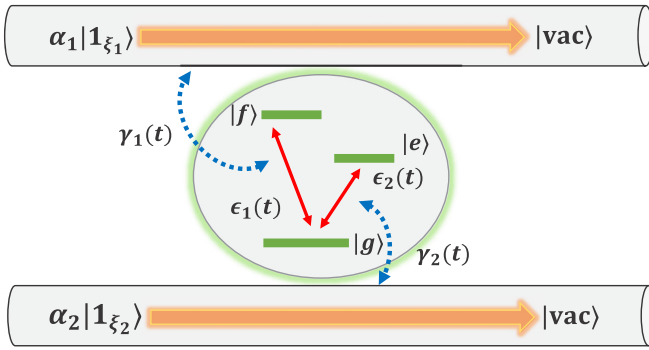


FIG. 8. Schematics for catching flying qubits at state $\alpha_1|1_{\xi_1}\rangle|vac\rangle + \alpha_2|vac\rangle|1_{\xi_2}\rangle$ by a V-type atom at state $|g\rangle$. Here $\epsilon_1(t)$ and $\epsilon_2(t)$ are the detuning frequencies between the incident field and the $|f\rangle \leftrightarrow |g\rangle$ and $|e\rangle \leftrightarrow |g\rangle$ transition frequencies, respectively. $\gamma_1(t)$ and $\gamma_2(t)$ are the coupling functions between the atom and the channels.

the entangled qubits to be caught by the three-level atom is

$$\gamma_k(t) = \frac{|\xi_k(t)|^2}{\int_{-\infty}^t |\xi_k(s)|^2 ds}, \quad \epsilon_k(t) = \dot{\phi}_k(t), \quad (32)$$

where $k = 1, 2$ (the derivation is straightforward and will not be provided here). Consequently, the entangled state is transferred to the atom's superposition state $\alpha_1|f\rangle + \alpha_2|e\rangle$.

The obtained solutions can still be interpreted by the rule of Eq. (31) and $\gamma_2(t) \equiv 0$, that is, the denominators are equal to the population of the associated excited state accumulated from the absorption of the corresponding single photon.

V. THE CONVERSION OF FLYING QUBITS BY A THREE-LEVEL ATOM

It is natural to use a Λ -type atom to convert a single photon between the two coupled channels. The conversion cannot only reshape the single photon but also change its carrier frequency [note that $\xi(t)$ is the envelope of the single-photon shape function in the rotating-wave frame].

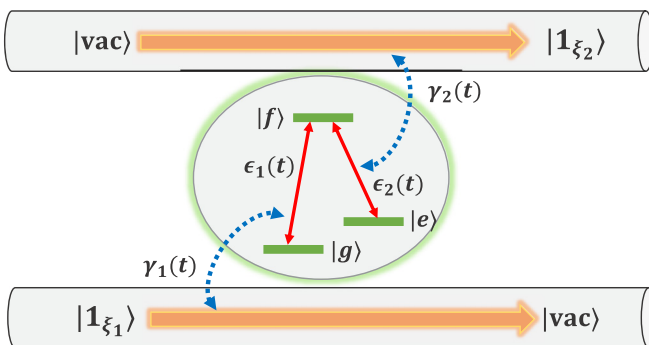


FIG. 9. Schematics for the conversion of flying qubits from state $|1_{\xi_1}\rangle|vac\rangle$ to $|vac\rangle|1_{\xi_2}\rangle$ by a Λ -type atom. Here $\epsilon_1(t)$ and $\epsilon_2(t)$ are the detuning frequencies between the incident field and the $|f\rangle \leftrightarrow |g\rangle$ and $|f\rangle \leftrightarrow |e\rangle$ transition frequencies, respectively. $\gamma_1(t)$ and $\gamma_2(t)$ are the coupling coefficients between the Λ -type atom and the channels.

As is shown in Fig. 9, we want to design control protocols such that the atom converts a single photon (at state $|1_{\xi_1}\rangle$) in the first channel to a single photon (at state $|1_{\xi_2}\rangle$) in the second channel. This consists of the catching of the first photon via transition from $|g\rangle$ to $|f\rangle$ and then the release of the second photon via transition from $|f\rangle$ to $|e\rangle$.

Similarly, we can introduce an ancillary system to generate $|1_{\xi_1}\rangle$ and obtain the conditions for the coupling functions and detuning frequencies to satisfy. In Appendix A 3 we derive that

$$\gamma_1(t) = \frac{|\xi_1(t)|^2}{\int_{-\infty}^t |\xi_1(\tau)|^2 d\tau - \int_{-\infty}^t |\xi_2(\tau)|^2 d\tau}, \quad (33)$$

$$\gamma_2(t) = \frac{|\xi_2(t)|^2}{\int_t^{\infty} |\xi_2(\tau)|^2 d\tau - \int_t^{\infty} |\xi_1(\tau)|^2 d\tau},$$

and the detuning frequencies are

$$\epsilon(t) = \dot{\phi}_1(t) = \dot{\phi}_2(t). \quad (34)$$

Moreover, for physically realizable conversions, the phase functions must satisfy

$$\phi_1(t) - \phi_2(t) = (2n + 1)\pi, \quad n \in \mathbb{Z}.$$

This is different from the phase condition for the generation of single photons.

It should be noted that the shape functions $\xi_1(t)$ and $\xi_2(t)$ for the desired conversion must also satisfy the condition (29) on the tail areas for physical realizability, otherwise the resulting coupling strength may become unphysically negative. This is because the outgoing photon must be released after the incoming photon is caught, or equivalently saying, the radiated energy into the outgoing photon must be less than the energy absorbed from the incoming photon. Their difference, as described by the common denominator in Eq. (33), is nothing but the gained population of the state $|f\rangle$ shared by the two channels. This again conforms to the population rule we observed in the above three control scenarios.

Hence, the shape of the incoming photon $\xi_1(t)$ must decay more quickly than that of the outgoing photon, and consequently, $\gamma_1(t)$ will asymptotically approach $\bar{\gamma}_1(t)$ (the solution for catching $|1_{\xi_2}\rangle$ with a two-level atom) when $t \rightarrow -\infty$, and $\gamma_2(t)$ will approach $\bar{\gamma}_2(t)$ (the solution for generating $|1_{\xi_2}\rangle$ with a two-level atom) when $t \rightarrow \infty$.

For demonstration, we test the same group of Gaussian shapes simulated in Sec. III, as the two cases are both subject to the physical realizability condition (29). As is shown in Figs. 10(a) and 10(c), the tail area condition is violated when the two pulses have different width but identical peak time, and thus the coupling functions $\gamma_1(t)$ and $\gamma_2(t)$ become nonphysical (i.e., negative) after the peak time. In Figs. 10(b) and 10(d), the resulting coupling functions are physically realizable when the two pulses have identical shapes but different peak times, and one can clearly observe the predicted asymptotic limits of $\gamma_1(t)$ and $\gamma_2(t)$ when $t \rightarrow \pm\infty$.

As a typical single-photon scattering process, the conversion of single photons can also be investigated via the scattering-matrix analysis proposed in Refs. [18,60]. The input-output relation of the shape functions can be expressed

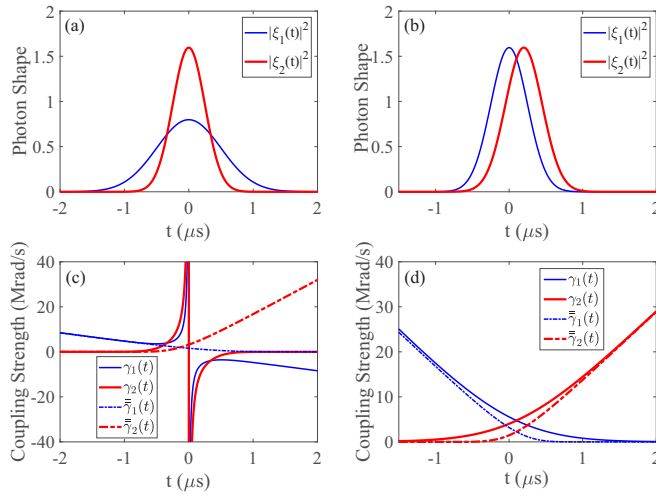


FIG. 10. The conversion of a flying qubit $|1_{\xi_1}\rangle$ in the first channel into a flying qubit $|1_{\xi_2}\rangle$ using a Λ -type atom. The incident photon shapes $\xi_1(t)$ and $\xi_2(t)$ are with (a) different Gaussian shapes or (b) same Gaussian shapes. The corresponding coupling strengths are shown in (c) and (d), respectively.

as follows:

$$\xi_2(t_2) = \int_{-\infty}^{t_2} S(t_2, t_1) \xi_1(t_1) dt_1, \quad (35)$$

where $S(t_2, t_1)$ is the scattering matrix defined in the time domain. The upper limit of the integral is set to t_2 owing to the causality of the input-output process [i.e., the value of $\xi_2(t_2)$ is only dependent on the past of $\xi_1(t)$].

According to Ref. [18], the scattering matrix can be calculated from (6) as follows:

$$S(t_2, t_1) = \langle e|V(\infty)\tilde{L}_2(t_2)\tilde{L}_1^\dagger(t_1)|g\rangle, \quad (36)$$

where $\tilde{L}_1^\dagger(t) = V^{-1}(t)L_1^\dagger(t)V(t)$. This gives

$$S(t_2, t_1) = \sqrt{\gamma_1(t_1)\gamma_2(t_2)} e^{-\frac{1}{2}\int_{t_1}^{t_2}\gamma(s)ds} e^{-i\int_{t_1}^{t_2}\epsilon(s)ds}, \quad (37)$$

where $\gamma(s) = \gamma_1(s) + \gamma_2(s)$ and $\epsilon(s) = \epsilon_1(s) + \epsilon_2(s)$.

Note that this scattering-matrix description is equivalent to the broadly adopted frequency-domain definition in the literature [60]. One can apply Fourier transform to rewrite (35) as

$$\hat{\xi}_2(\omega_2) = \int_{-\infty}^{\infty} \hat{S}(\omega_2, \omega_1) \hat{\xi}_1(\omega_1) d\omega_1, \quad (38)$$

where $\hat{\xi}_1(\omega_1)$, $\hat{\xi}_2(\omega_2)$, and $\hat{S}(\omega_2, \omega_1)$ are the Fourier transform of $\xi_1(t_1)$, $\xi_2(t_2)$, and $S(t_2, t_1)$, with

$$\hat{S}(\omega_2, \omega_1) = \int_{-\infty}^{\infty} dt_2 \int_{-\infty}^{t_2} dt_1 S(t_2, t_1) e^{-i\omega_1 t_1 - i\omega_2 t_2}. \quad (39)$$

We visualize the scattering matrices under the coupling functions (33) designed for the conversion of Gaussian-shape single-photon pulses shown in Fig. 10(b). As are shown in Fig. 11, the resulting scattering matrices are displayed on the domain of definition $\{(t_1, t_2) : t_1 \leq t_2\}$, which all appear in Gaussian shapes. Their peaks are located on the t_2 axis (i.e., with $t_1 = 0$) and move away from the origin when the time delay Δ increases, and their widths are determined by

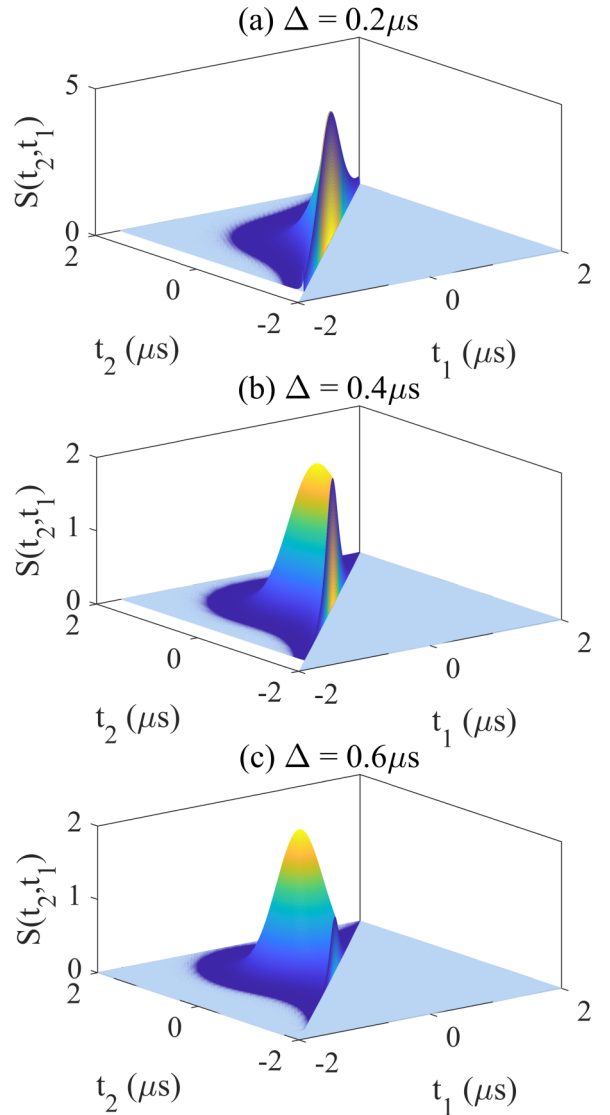


FIG. 11. The scattering matrices for conversion of Gaussian-shape single photons with time delays $\Delta = 0.2, 0.4$, and $0.6 \mu\text{s}$, respectively. The scattering matrices are defined in the region $t_2 \geq t_1$.

the width of the input and output pulses in Fig. 10(b). It should be noted that the resulting scattering process can only perfectly convert the selected Gaussian-shape function $\xi_1(t)$ into a single-photon pulse, because the coupling functions (33) is determined by $\xi_1(t)$. When the shape of the input photon changes (e.g., a narrower or broader Gaussian pulse), the number of photons in the output field is still unit owing to the preservation of energy. However, as can be verified in our numerical simulations, the photon field is not entirely scattered into the second channel because a part of the field may go into the other channel.

VI. THE BUNCHING AND ANTIBUNCHING OF PHOTONS

To better understand the above control processes, this section will study the correlation properties [50,61] of the output fields, which are broadly applied to characterize the nonclassical features of photon fields. The photon shapes

discussed above can be taken as the first-order property defined as the correlation of field amplitudes at different time instants. The correlation of photon numbers, which corresponds to the second-order correlation, are important for qualifying few-photon resources via their bunching or antibunching characteristics. In the following, we will investigate the second-order correlation of emitted photon fields in the above examples.

Let $|\eta\rangle$ be the joint state of the output photon fields in the two channels coupled to the three-level atom. The second-order correlation functions [61,62] are defined as follows:

$$G_{i,k}^{(2)}(\tau) = \int_{-\infty}^{\infty} dt \langle \eta | b_i^\dagger(t) b_k^\dagger(t + \tau) b_k(t + \tau) b_i(t) | \eta \rangle, \quad (40)$$

where $i, k = 1, 2$, which represents to the probability of observing a photon in the k th channel at time delay τ after a photon is emitted into the i th channel. Thus, the factorizable second-order correlation functions [61,62] could be written as

$$\bar{G}_{i,k}^{(2)}(\tau) = \int_{-\infty}^{\infty} dt \langle \eta | b_i^\dagger(t) b_i(t) | \eta \rangle \langle \eta | b_k^\dagger(t + \tau) b_k(t + \tau) | \eta \rangle. \quad (41)$$

The photon field is said to be antibunching if

$$G_{i,k}^{(2)}(0) < \bar{G}_{i,k}^{(2)}(0), \quad (42)$$

which implies that photons are less likely to simultaneously appear in the i th and k th channel owing to the effective repulsive photon-photon coupling induced by the atom. Otherwise, if

$$G_{i,k}^{(2)}(0) > \bar{G}_{i,k}^{(2)}(0), \quad (43)$$

the field is called bunching, meaning that the photons tend to appear simultaneously in the i th and k th channel owing to the effective attractive photon-photon coupling induced by the atom [61,62].

To calculate the explicit form of the correlation functions, we need the following property:

$$b_{j_1}(t_1) \cdots b_{j_n}(t_n) | n_\xi \rangle = \xi_{j_1, \dots, j_n}(t_1, \dots, t_n) | \text{vac} \rangle \quad (44)$$

that can be easily verified, where the n -photon state $|n_\xi\rangle$ is defined by Eq. (4). Using these properties, we can calculate the correlation functions in all cases discussed above. For example, in the generation of entangled flying qubits discussed in Sec. III A, we can derive that all second-order correlation functions $G_{i,k}^{(2)}(\tau) \equiv 0$ for all $i, k = 1, 2$, exhibiting intrinsic antibunching of photons. This is because the two output channels share only one photon, which leaves no chance for observing a second photon after the first photon is emitted.

The bunching of photons can be observed in the cascaded generation of correlated photon pairs that are sequentially emitted to the first and second channels, respectively, discussed in Sec. III B. Physically, this implies that photon bunching is possible in the cross-correlation functions $G_{1,2}^{(2)}(\tau)$ and $G_{2,1}^{(2)}(\tau)$. Also, photon antibunching will be observed in the autocorrelation functions $G_{1,1}^{(2)}(\tau)$ and $G_{2,2}^{(2)}(\tau)$ as the two photons can be never be found in the same channel.

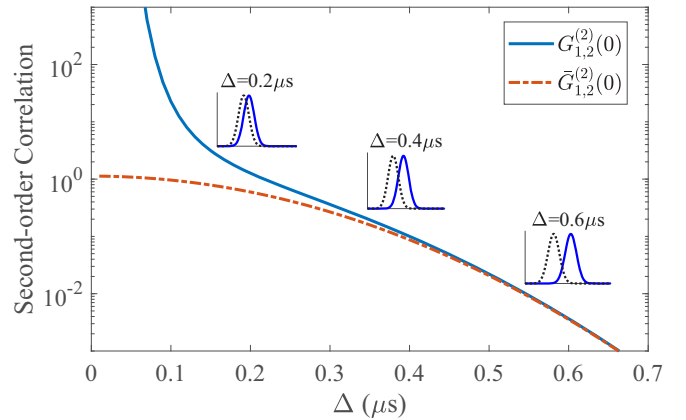


FIG. 12. The curves $G_{1,2}^{(2)}(0)$ and $\bar{G}_{1,2}^{(2)}(0)$ when varying the separation time Δ between the emitted photon pulses $\xi_1(t)$ and $\xi_2(t)$. Strong bunching of photons appears when Δ is small. The three insets are the Gaussian shapes as $\Delta = 0.2 \mu\text{s}$, $\Delta = 0.4 \mu\text{s}$, and $\Delta = 0.6 \mu\text{s}$, respectively.

These predictions can be verified from the calculation using the property (44), which indicates that $G_{1,1}^{(2)}(\tau) = G_{2,2}^{(2)}(\tau) \equiv 0$. The cross-correlation function

$$G_{1,2}^{(2)}(\tau) = \int_{-\infty}^{\infty} dt |\xi_{1,2}^g(t, t + \tau)|^2, \quad (45)$$

where $|\xi_{1,2}^g(t_1, t_2)\rangle$ is the wave packet function of the cascaded two-photon emission given by (25). The corresponding factorizable correlation function

$$\bar{G}_{1,2}^{(2)}(\tau) = \int_{-\infty}^{\infty} dt |\xi_1(t)|^2 |\xi_2(t + \tau)|^2, \quad (46)$$

where the single-photon wave packets $\xi_1(t)$ and $\xi_2(t)$ are defined by Eqs. (26) and (27), respectively.

To illustrate the above results, we simulate the second-order cross-correlation functions for the Gaussian-shape two-photon pulses generated by a Ξ -type atom, which is displayed in Fig. 5(b). Both $G_{1,2}^{(2)}(0)$ and $\bar{G}_{1,2}^{(2)}(0)$ are calculated according to Eqs. (45) and (46) with the separation time Δ increasing from 0 to $0.7 \mu\text{s}$. As is shown in Fig. 12, the curve of $G_{1,2}^{(2)}(0)$ is always above $\bar{G}_{1,2}^{(2)}(0)$, exhibiting typical photon bunching behavior due to the effective attractive photon-photon interaction induced by the atom. In particular, the photon bunching becomes very strong when the separation time Δ between the two averaged single-photon pulses $\xi_1(t)$ and $\xi_2(t)$ is very small (i.e., when the two pulses largely overlap with each other in the time domain).

VII. CONCLUSION AND OUTLOOK

To conclude, we have explored the control of flying qubits using various types of three-level atoms through tunable couplings to two input-output channels, including the generation of entangled qubits and correlated flying qubits, as well as the

catching and conversion of single flying qubits. Analytic formulas are presented for the coupling and detuning functions to fulfill these control tasks, which lay a basis for systematic design of control protocols for high-fidelity flying-qubit transmission over complex quantum networks.

It can be seen that in many cases the resulting coupling strengths tend to be infinitely strong when the time $t \rightarrow \pm\infty$, which is apparently physically unrealizable. Nonetheless, as long as the shape function of the output photon field has sufficiently decayed before the coupling strength gets too strong, we can cut off the coupling function or keep its strength at some saturated value.

The method applied here can be naturally generalized to more complicated cases that include more atomic levels and input-output channels, as long as the number of excitations (or energy) is preserved. We conjecture that, owing to the conservation law, the population rule concluded in this paper will still hold, i.e., the flying-qubit control problems can be decomposed into several single-photon generation or catching problems, and the corresponding coupling function is equal to the ratio between the square norm of the desired photon shape and the current population of the excited state associated with this photon. This rule can be verified by Eqs. (17), (28), and (31)–(33) for control protocols using a two-level or three-level atom. Whether this holds for most general cases is to be examined in our future studies.

In addition to the three types of three-level atoms we studied here, it is more intriguing to apply a Δ -type atom, which is only realizable by artificial atoms, for the control of flying qubits. For example, one can use it to convert a single photon into a pair of correlated photon pair, or vice versa, or routing a single photon between two different channels. However, the underlying scattering process is much more complicated, and we have not obtained any useful analytic solutions.

Furthermore, the correlation properties of the output fields, such as the bunching and antibunching of photons, has been discussed after the various controls of flying qubits above.

It should be noted that the obtained solutions may confront physical constraints on the realizable shape functions $\xi_1(t)$ and $\xi_2(t)$, such as the phase conditions and the restriction (29) on the pulse tail areas. Towards more flexible flying-qubit shaping controls, one may have to introduce coherent controls that break the conservation of the number of excitations. Under such circumstances, analytic solutions are usually unavailable, but numerical optimization methods can be introduced to assist the design. All these problems will be explored in our future studies.

ACKNOWLEDGMENTS

This work is supported by the National Natural Science Foundation of China under Grants No. 61833010, No. 62173201, and No. 6217023269. G.Z. acknowledges supports from the Hong Kong Research Grant Council (RGC) Grants No. 15203619 and No. 15208418, the Shenzhen Fundamental Research Program under Grant No. JCYJ20190813165207290, and the CAS AMSS-PolyU Joint Laboratory of Applied Mathematics.

APPENDIX: PROOFS OF MAIN RESULTS

For conciseness, we introduce several notations as follows:

$$\Gamma_j(t) = \int_{-\infty}^t \gamma_j(\tau) d\tau, \quad (\text{A1})$$

$$\Theta_j(t) = \int_{-\infty}^t \epsilon_j(\tau) d\tau, \quad (\text{A2})$$

where $\gamma_j(\tau)$ and $\epsilon_j(\tau)$ ($j = 1, 2$) are the coupling and detuning functions of the j th channel. Based on the above notations, we further denote $\gamma(t) = \gamma_1(t) + \gamma_2(t)$ and $\epsilon(t) = \epsilon_1(t) + \epsilon_2(t)$. $\Gamma(t) = \Gamma_1(t) + \Gamma_2(t)$ and $\Theta(t) = \Theta_1(t) + \Theta_2(t)$ can be obtained.

In the following we will prove the main results presented in the main text.

1. The derivation of Eqs. (17) and (18)

Applying Eqs. (6)–(9), it is straightforward to find that, with the Hamiltonian and coupling operator given in Sec. III A, only the single-photon emissions can occur when the three-level atom is initially prepared at $|f\rangle$ and ends up in $|g\rangle$ or $|e\rangle$. The calculation of Eq. (8) on the single-photon emission gives

$$\xi_1^g(\tau) = \sqrt{\gamma_1(\tau)} e^{-\frac{1}{2}\Gamma(s) - i\Theta(s)}, \quad (\text{A3})$$

$$\xi_2^e(\tau) = \sqrt{\gamma_2(\tau)} e^{-\frac{1}{2}\Gamma(s) - i\Theta(s)}. \quad (\text{A4})$$

To generate the target distributed single photon that are entangled with the atom at state $\alpha_1|g\rangle|1_{\xi_1}\rangle|\text{vac}\rangle + \alpha_2|e\rangle|\text{vac}\rangle|1_{\xi_2}\rangle$, the relations $\xi_1^g(\tau) = \alpha_1\xi_1(\tau)$ and $\xi_2^e(\tau) = \alpha_2\xi_2(\tau)$ should be established, and hence

$$\alpha_1\xi_1(\tau) = \sqrt{\gamma_1(\tau)} e^{-\frac{1}{2}\Gamma(s) - i\Theta(s)}, \quad (\text{A5})$$

$$\alpha_2\xi_2(\tau) = \sqrt{\gamma_2(\tau)} e^{-\frac{1}{2}\Gamma(s) - i\Theta(s)}. \quad (\text{A6})$$

Let $\xi_k(\tau) = |\xi_k(\tau)|e^{-i\phi_k(\tau)}$, $k = 1, 2$. The phase condition Eq. (18) can be immediately obtained by comparing the phases of the left- and right-hand sides of Eqs. (A5) and (A6). These two equations also imply

$$\frac{|\alpha_1\xi_1(\tau)|^2}{|\alpha_2\xi_2(\tau)|^2} = \frac{\gamma_1(\tau)}{\gamma_2(\tau)} \quad (\text{A7})$$

and

$$|\alpha_1\xi_1(\tau)|^2 + |\alpha_2\xi_2(\tau)|^2 = \gamma(\tau)e^{-\Gamma(\tau)} = -\frac{d}{d\tau}e^{-\Gamma(\tau)}. \quad (\text{A8})$$

The integration of both sides of Eq. (A8) from $-\infty$ to t gives

$$\int_{-\infty}^t [|\alpha_1\xi_1(\tau)|^2 + |\alpha_2\xi_2(\tau)|^2] d\tau = -e^{-\Gamma(t)}, \quad (\text{A9})$$

from which we solve

$$\gamma(t) = \frac{|\alpha_1\xi_1(t)|^2 + |\alpha_2\xi_2(t)|^2}{\int_{-\infty}^t [|\alpha_1\xi_1(\tau)|^2 + |\alpha_2\xi_2(\tau)|^2] d\tau}. \quad (\text{A10})$$

The solution (17) of $\gamma_1(t)$ and $\gamma_2(t)$ can thus be obtained by (A7) and (A10).

2. The derivation of Eq. (28)

We apply Eqs. (6)–(9) with the model of Ξ -type atom described in Sec. III B. According to the definitions (A11) and (A12), we derive that

$$|\xi_1(\tau_1)|^2 = \int_{\tau_1}^{\infty} |\xi_{1,2}^g(\tau_1, \tau_2)|^2 d\tau_2 = \gamma_1(\tau_1)e^{-\Gamma_1(\tau_1)}, \quad (\text{A11})$$

which can be simplified to obtain (Eq. (28a)) for the solution of $\gamma_1(t)$ and

$$\begin{aligned} |\xi_2(\tau_2)|^2 &= \int_{-\infty}^{\tau_2} |\xi_{1,2}^g(\tau_1, \tau_2)|^2 d\tau_1 \\ &= \gamma_2(\tau_2)e^{-\Gamma_2(\tau_2)} \int_{-\infty}^{\tau_2} |\xi_1(\tau_1)|^2 e^{\Gamma_2(\tau_1)} d\tau_1. \end{aligned} \quad (\text{A12})$$

As for the solution of $\gamma_2(t)$, we can rewrite Eq. (A12) as

$$\int_{-\infty}^{\tau_2} |\xi_1(\tau_1)|^2 e^{\Gamma_2(\tau_1)} d\tau_1 = \frac{|\xi_2(\tau_2)|^2}{\gamma_2(\tau_2)} e^{\Gamma_2(\tau_2)}, \quad (\text{A13})$$

and differentiate both sides of Eq. (A13) to obtain the solution ((28b)).

3. The derivation of Eqs. (33) and (34)

We first construct an auxiliary system A to virtually generate the incident single photon $|1_{\xi_1}\rangle$, for which one can set

$$H_A(t) = 0, \quad L_A(t) = \sqrt{\gamma_A(t)}\sigma_-, \quad (\text{A14})$$

with the coupling function being

$$\gamma_A(t) = \frac{|\xi_1(t)|^2}{\int_t^{\infty} |\xi_1(s)|^2 ds}, \quad (\text{A15})$$

where $\gamma_A(t)$ is the coupling function between the auxiliary system and the first channel. According to the (S, L, H) formula [59], the equivalent Hamiltonian of the joint system as Eq. (10) is

$$\begin{aligned} \bar{H}(t) &= \mathbb{I}_A \otimes [\epsilon_1(t) + \epsilon_2(t)]|f\rangle\langle f| \\ &+ \frac{1}{2i}\sqrt{\gamma_A(t)\gamma_1(t)}[|g, f\rangle\langle e, g| - \text{H.c.}], \end{aligned} \quad (\text{A16})$$

where the notation $|\alpha, \beta\rangle = |\alpha\rangle \otimes |\beta\rangle$ is adopted. The corresponding equivalent coupling operators as Eq. (11) are

$$\begin{aligned} \bar{L}_1(t) &= \mathbb{I}_A \otimes \sqrt{\gamma_1(t)}|g\rangle\langle f| + \sqrt{\gamma_A(t)}|g\rangle\langle e| \otimes \mathbb{I}, \\ \bar{L}_2(t) &= \mathbb{I}_A \otimes \sqrt{\gamma_2(t)}|e\rangle\langle f|. \end{aligned} \quad (\text{A17})$$

Applying Eq. (7) with the above equivalent $\bar{H}(t)$ and $\bar{L}_j(t)$, we can see that only the following three components of corre-

lated system states are nonvanishing:

$$\begin{aligned} |\psi(t)\rangle &= e^{-\frac{1}{2}\Gamma_A(t)}|e, g\rangle - \Xi(t)e^{-\frac{1}{2}\Gamma(t)}|g, f\rangle, \\ |\psi_1(\tau|t)\rangle &= [\xi_1(\tau) - \sqrt{\gamma_1(\tau)}e^{-\frac{1}{2}\Gamma(\tau)-i\Theta(\tau)}\Xi(\tau)]|g, g\rangle, \\ |\psi_2(\tau|t)\rangle &= -\sqrt{\gamma_2(\tau)}e^{-\frac{1}{2}\Gamma(\tau)-i\Theta(\tau)}\Xi(\tau)|g, e\rangle, \end{aligned} \quad (\text{A18})$$

where $\Gamma_A(t) = \int_{-\infty}^t \gamma_A(s)ds$ and

$$\Xi(t) = \int_{-\infty}^t \sqrt{\gamma_1(\tau)}e^{\frac{1}{2}\Gamma(\tau)+i\Theta(\tau)}\xi_1(\tau)d\tau. \quad (\text{A19})$$

The three nonvanishing components correspond to the cases when both channels have vacuum output, the first channel has a single-photon output, and the second channel has a single-photon output, respectively.

Note that $|\psi_1(\tau|t)\rangle$ and $|\psi_2(\tau|t)\rangle$ are both independent of t , and hence we have

$$\xi_1^g(\tau) = \xi_1(\tau) - \sqrt{\gamma_1(\tau)}e^{-\frac{1}{2}\Gamma(\tau)-i\Theta(\tau)}\Xi(\tau), \quad (\text{A20})$$

$$\xi_2^e(\tau) = -\sqrt{\gamma_2(\tau)}e^{-\frac{1}{2}\Gamma(\tau)-i\Theta(\tau)}\Xi(\tau). \quad (\text{A21})$$

To convert the incident flying qubit $|1_{\xi_1}\rangle$ into the outgoing flying qubit $|1_{\xi_2}\rangle$, the single photon must completely go out through the second channel, and hence $\xi_1^g(\tau) = 0$ and $\xi_1^e(\tau) = \xi_2(\tau)$, which implies that the two shape functions satisfy

$$\xi_1(\tau) = \sqrt{\gamma_1(\tau)}e^{-\frac{1}{2}\Gamma(\tau)-i\Theta(\tau)}\Xi(\tau), \quad (\text{A22})$$

$$\xi_2(\tau) = -\sqrt{\gamma_2(\tau)}e^{-\frac{1}{2}\Gamma(\tau)-i\Theta(\tau)}\Xi(\tau). \quad (\text{A23})$$

Now we apply the normalization condition of the atom-field joint state (5), which requires that

$$\begin{aligned} 1 &\equiv \langle\Psi(t)|\Psi(t)\rangle = \langle\psi(t)|\psi(t)\rangle \\ &+ \int_{-\infty}^t [\langle\psi_1(\tau|t)|\psi_1(\tau|t)\rangle + \langle\psi_2(\tau|t)|\psi_2(\tau|t)\rangle]d\tau. \end{aligned} \quad (\text{A24})$$

Combining with Eqs. (A18), (A22), and (A23), we can transform Eq. (A24) as follows:

$$1 \equiv \int_t^{\infty} |\xi_1(\tau)|^2 d\tau + |\Xi(t)|^2 e^{-\Gamma(t)} + \int_{-\infty}^t |\xi_2(\tau)|^2 d\tau, \quad (\text{A25})$$

where the relation $e^{-\Gamma_A(t)} = \int_t^{\infty} |\xi_1(s)|^2 ds$ is used.

This equation precisely describes the conservation of the number of excitations (or energy in the joint system). The system is initially prepared at the ground state with a single-photon input, and hence its total number of excitations is 1, as indicated by the left-hand side of Eq. (A25). At any time $t > 0$, the energy contained in the photon may stay in the input field (the first term on the right-hand side) or be transferred to the population of $|f\rangle$ (the second term on the right-hand side) and the output field (the third term on the right-hand side). When $t \rightarrow \infty$, all the energy flows from the incoming photon to the outgoing photon, while the first and second terms decay to zero.

Furthermore, Eq. (A25) implies that

$$\begin{aligned} |\Xi(t)|^2 e^{-\Gamma(t)} &= \int_{-\infty}^t |\xi_1(\tau)|^2 d\tau - \int_{-\infty}^t |\xi_2(\tau)|^2 d\tau \\ &= \int_t^{\infty} |\xi_2(\tau)|^2 d\tau - \int_t^{\infty} |\xi_1(\tau)|^2 d\tau, \end{aligned} \quad (\text{A26})$$

as both $\xi_1(\tau)$ and $\xi_2(\tau)$ are normalized functions. Replacing this equation back into Eqs. (A22) and (A23), we obtain the solutions for the coupling functions:

$$\begin{aligned} \gamma_1(t) &= \frac{|\xi_1(t)|^2}{\int_{-\infty}^t |\xi_1(\tau)|^2 d\tau - \int_{-\infty}^t |\xi_2(\tau)|^2 d\tau}, \\ \gamma_2(t) &= \frac{|\xi_2(t)|^2}{\int_t^{\infty} |\xi_2(\tau)|^2 d\tau - \int_t^{\infty} |\xi_1(\tau)|^2 d\tau}. \end{aligned} \quad (\text{A27})$$

As for the solutions of the detuning functions, one can directly observe that Eqs. (A22) and (A23) are satisfied when

$$\epsilon(t) = \dot{\phi}_1(t), \quad \epsilon(t) = \dot{\phi}_2(t), \quad (\text{A28})$$

where $\phi_1(t)$ and $\phi_2(t)$ are the phase functions of $\xi_1(t)$ and $\xi_2(t)$, respectively. Moreover, Eqs. (A22) and (A23) indicate that $\xi_1(t)$ and $\xi_2(t)$ must have inverted phases, i.e.,

$$\phi_1(t) - \phi_2(t) = (2n + 1)\pi, \quad n \in \mathbb{Z}.$$

The obtained equations also provide the solution for catching an incident single photon from the first channel, which requires that $\xi_1^g(\tau) = \xi_2^e(\tau) = 0$. According to Eq. (A23), $\gamma_2(t)$ must be turned off so that the resulting design is equivalent to that with a two-level atom.

-
- [1] D. Divincenzo, *Science* **270**, 255 (1995).
[2] J. I. Cirac, P. Zoller, H. J. Kimble, and H. Mabuchi, *Phys. Rev. Lett.* **78**, 3221 (1997).
[3] H. J. Kimble, *Nature (London)* **453**, 1023 (2008).
[4] A. Kuhn, M. Hennrich, and G. Rempe, *Phys. Rev. Lett.* **89**, 067901 (2002).
[5] L. Duan, M. D. Lukin, J. I. Cirac, and P. Zoller, *Nature (London)* **414**, 413 (2001).
[6] K. Gheri, K. Ellinger, T. Pellizzari, and P. Zoller, *Fortschr. Phys.* **46**, 401 (1998).
[7] Y. Wang, J. Minar, L. Sheridan, and V. Scarani, *Phys. Rev. A* **83**, 063842 (2011).
[8] S. A. Aljunid, G. Maslennikov, Y. Wang, H. L. Dao, V. Scarani, and C. Kurtsiefer, *Phys. Rev. Lett.* **111**, 103001 (2013).
[9] H. I. Nurdin, M. R. James, and N. Yamamoto, in *55th IEEE Conference on Decision and Control (CDC)* (2016), pp. 2513–2518.
[10] C. W. Gardiner and M. J. Collett, *Phys. Rev. A* **31**, 3761 (1985).
[11] J. Combes, J. Kerckhoff, and M. Sarovar, *Adv. Phys.: X* **2**, 784 (2017).
[12] G. Zhang, *Control Theory Technol.* **19**, 544 (2021).
[13] C. Kurtsiefer, S. Mayer, P. Zarda, and H. Weinfurter, *Phys. Rev. Lett.* **85**, 290 (2000).
[14] A. Houck, D. Schuster, J. Gambetta, J. Schreier, B. Johnson, J. Chow, L. Frunzio, J. Majer, M. Devoret, S. Girvin *et al.*, *Nature (London)* **449**, 328 (2007).
[15] M. Pierre, I. Svensson, S. Sathyamoorthy, G. Johansson, and P. Delsing, *Appl. Phys. Lett.* **104**, 232604 (2014).
[16] J. Gough and G. Zhang, *EPJ Quantum Technol.* **2**, 15 (2015).
[17] P. Forn-Diaz, C. W. Warren, C. W. S. Chang, A. M. Vadiraj, and C. M. Wilson, *Phys. Rev. Appl.* **8**, 054015 (2017).
[18] R. Trivedi, K. Fischer, S. Xu, S. Fan, and J. Vuckovic, *Phys. Rev. B* **98**, 144112 (2018).
[19] K. Fischer, R. Trivedi, V. Ramasesh, I. Siddiqi, and J. Vučković, *Quantum* **2**, 69 (2018).
[20] M. Stobinska, G. Alber, and G. Leuchs, *Europhys. Lett.* **86**, 14007 (2009).
[21] Y. Yin, Y. Chen, D. Sank, P. J. J. O’Malley, T. C. White, R. Barends, J. Kelly, E. Lucero, M. Mariantoni, A. Megrant, C. Neill, A. Vainsencher, J. Wenner, A. N. Korotkov, A. N. Cleland, and J. M. Martinis, *Phys. Rev. Lett.* **110**, 107001 (2013).
[22] D. L. Sounas, *Phys. Rev. B* **101**, 104303 (2020).
[23] G. Zhang, *Automatica* **50**, 442 (2014).
[24] G. Zhang, *Automatica* **83**, 186 (2017).
[25] V. Leong, M. Seidler, M. Steiner, A. Cere, and C. Kurtsiefer, *Nat. Commun.* **7**, 13716 (2016).
[26] D. L. Hurst and P. Kok, *Phys. Rev. A* **97**, 043850 (2018).
[27] A. H. Kiilerich and K. Mølmer, *Phys. Rev. Lett.* **123**, 123604 (2019).
[28] W.-L. Li, G. Zhang, and R.-B. Wu, *IFAC-PapersOnLine* **53**, 299 (2020), 21st IFAC World Congress.
[29] W.-L. Li, G. Zhang, and R.-B. Wu, *Automatica* **143**, 110338 (2022).
[30] H. Song, G. Zhang, and Z. Xi, *SIAM J. Control Optim.* **54**, 1602 (2016).
[31] Z. Dong, G. Zhang, and N. H. Amini, *Quant. Info. Proc.* **18**, 136 (2019).
[32] Z. Dong, G. Zhang, and N. H. Amini, *SIAM J. Control Optim.* **57**, 3445 (2019).
[33] Y. Pan, G. Zhang, and M. R. James, *Automatica* **69**, 18 (2016).
[34] Y. Pan and G. Zhang, *J. Phys. A: Math. Theor.* **50**, 345301 (2017).
[35] E. Schöll, L. Schweickert, L. Hanschke, K. D. Zeuner, F. Sbresny, T. Lettner, R. Trivedi, M. Reindl, S. F. C. da Silva, R. Trotta *et al.*, *Phys. Rev. Lett.* **125**, 233605 (2020).
[36] F. Sbresny, L. Hanschke, E. Schöll, W. Rauhaus, B. Scaparra, K. Boos, E. Zubizarreta Casalengua, H. Riedl, E. del Valle, J. J. Finley *et al.*, *Phys. Rev. Lett.* **128**, 093603 (2022).
[37] Y.-x. Liu, J. Q. You, L. F. Wei, C. P. Sun, and F. Nori, *Phys. Rev. Lett.* **95**, 087001 (2005).
[38] Z. H. Peng, S. E. D. Graaf, J. S. Tsai, and O. V. Astafiev, *Nat. Commun.* **7**, 12588 (2016).
[39] X. Gu, A. Kockum, A. Miranowicz, Y.-x. Liu, and F. Nori, *Phys. Rep.* **718-719**, 1 (2017).
[40] V. E. Manucharyan, J. Koch, L. I. Glazman, and M. H. Devoret, *Science* **326**, 113 (2009).
[41] A. A. Abdumalikov, O. Astafiev, A. M. Zagoskin, Y. A. Pashkin, Y. Nakamura, and J. S. Tsai, *Phys. Rev. Lett.* **104**, 193601 (2010).

- [42] S. J. Srinivasan, A. J. Hoffman, J. M. Gambetta, and A. A. Houck, *Phys. Rev. Lett.* **106**, 083601 (2011).
- [43] J. Q. You, Y.-x. Liu, C. P. Sun, and F. Nori, *Phys. Rev. B* **75**, 104516 (2007).
- [44] O. Astafiev, K. Inomata, A. O. Niskanen, T. Yamamoto, Y. A. Pashkin, Y. Nakamura, and J. S. Tsai, *Nature (London)* **449**, 588 (2007).
- [45] C. Gonzalez-Ballester, E. Moreno, F. J. Garcia-Vidal, and A. Gonzalez-Tudela, *Phys. Rev. A* **94**, 063817 (2016).
- [46] O. Kyriienko and A. S. Sørensen, *Phys. Rev. Lett.* **117**, 140503 (2016).
- [47] F. Marquardt, *Phys. Rev. B* **76**, 205416 (2007).
- [48] Z. H. Peng, Y.-x. Liu, J. T. Peltonen, T. Yamamoto, J. S. Tsai, and O. Astafiev, *Phys. Rev. Lett.* **115**, 223603 (2015).
- [49] L. Zhou, L.-P. Yang, Y. Li, and C. P. Sun, *Phys. Rev. Lett.* **111**, 103604 (2013).
- [50] M. Scully and M. Zubairy, *Quantum Optics* (Cambridge University Press, New York, 1997).
- [51] H. Carmichael, *An Open Systems Approach to Quantum Optics* (Springer, Berlin, 1993).
- [52] J. Gough, M. James, and H. Nurdin, *New J. Phys.* **16**, 075008 (2014).
- [53] T. Shi, D. E. Chang, and J. I. Cirac, *Phys. Rev. A* **92**, 053834 (2015).
- [54] J.-T. Shen and S. Fan, *Phys. Rev. Lett.* **98**, 153003 (2007).
- [55] Y. Pan, D. Dong, and G. Zhang, *New J. Phys.* **18**, 033004 (2016).
- [56] Y.-X. Liu, H.-C. Sun, Z. Peng, A. Miranowicz, J. Tsai, and F. Nori, *Sci. Rep.* **4**, 7289 (2014).
- [57] H. Zheng, D. J. Gauthier, and H. U. Baranger, *Phys. Rev. A* **85**, 043832 (2012).
- [58] C. Gardiner and P. Zoller, *Quantum Noise* (Springer, Berlin, 2004).
- [59] J. Gough and M. R. James, *IEEE Trans, Automatic Control* **54**, 2530 (2009).
- [60] S. Fan, i. m. c. E. Kocabaş, and J.-T. Shen, *Phys. Rev. A* **82**, 063821 (2010).
- [61] D. Bozyigit, C. Lang, L. Steffen, J. M. Fink, C. Eichler, M. Baur, R. Bianchetti, P. J. Leek, S. Filipp, M. P. da Silva *et al.*, *Nat. Phys.* **7**, 154 (2011).
- [62] Y. Shih, *An Introduction to Quantum Optics: Photon and Biphoton Physics* (CRC, Boca Raton, FL, 2020).